

Research



Cite this article: Nieto-Vesperinas M. 2017 Chiral optical fields: a unified formulation of helicity scattered from particles and dichroism enhancement. *Phil. Trans. R. Soc. A* **375**: 20160314.
<http://dx.doi.org/10.1098/rsta.2016.0314>

Accepted: 4 October 2016

One contribution of 15 to a theme issue
'New horizons for nanophotonics'.

Subject Areas:

optics

Keywords:

electromagnetic helicity, dichroism, scattering

Author for correspondence:

Manuel Nieto-Vesperinas
e-mail: mnieto@icmm.csic.es

Chiral optical fields: a unified formulation of helicity scattered from particles and dichroism enhancement

Manuel Nieto-Vesperinas

Instituto de Ciencia de Materiales de Madrid, Consejo Superior de Investigaciones Científicas, Campus de Cantoblanco, Madrid 28049, Spain

 MN-V, 0000-0002-8957-6123

We establish a general unified formulation which, using the optical theorem of electromagnetic helicity, shows that dichroism is a phenomenon arising in any scattering—or diffraction—process, elastic or not, of chiral electromagnetic fields by objects either chiral or achiral. It is shown how this approach paves the way to overcoming well-known limitations of standard circular dichroism, like its weak signal or the difficulties of using it with magnetodielectric particles. Based on the angular spectrum, representation of optical fields with only right circular or left circular plane waves, we introduce beams with transverse elliptic polarization and possessing a longitudinal component. Then, our formulation for general optical fields shows how to enhance the extinction rate of incident helicity (and therefore the dichroism signal) versus that of energy of the light scattered or emitted by a particle, or vice versa.

This article is part of the themed issue 'New horizons for nanophotonics'.

1. Introduction

Chiral fields are acquiring increasing attention due to their potential as probes of matter at the nanoscale [1–9], of which life molecules are of paramount importance, or as high information capacity signals in communication channels [8,10–13] with control and transfer of angular momentum, which includes recently developed structured materials and metasurfaces. The conservation of the electromagnetic *helicity* of wavefields (or, equivalently, *chirality* when they are quasi-monochromatic; we shall

indistinctly use both terms for such fields) [4,6,14,15] was recently shown [16] to lead to a new *optical theorem* which characterizes the excitation and emission of field helicity—or chirality—by bodies, and that we believe should play a growing relevant role in coming years with the progress of research on applications of twisted light.

In this context, we pointed out [16] that *circular dichroism* (CD) [17–19], i.e. the difference in absorption—or emission—of energy by molecular objects according to the handedness of circularly polarized light (CPL), is a particular case of this optical theorem for scatterers, and hence it does not need to resort to quantum mechanics as usually done in its standard formulation. Thus, this phenomenon is just a consequence of the conservation of helicity of electromagnetic fields on scattering.

Different studies have discussed what kind of structures are necessary to produce chiral fields and whether CD requires those objects being chiral. However, some works have recently shown that this effect can be obtained with achiral objects [20]. Moreover, separating the existence of chirality from dichroism effects may be a problem in some observations [21,22]. Nonetheless no general and unified framework, not limited to particular structures, has been yet established.

In this paper, we show that dichroism is not only an effect due to absorption and e.g. fluorescent re-emission by molecules; but it constitutes a property of any scattering interaction, elastic or not, of electromagnetic twisted fields. Thus, based on the aforementioned optical theorem for the helicity, we generalize the concept of dichroism and demonstrate how it appears not only with CPL waves, but also with arbitrary chiral optical fields. This allows the design of an illumination that enhances the information content of the scattered signal, overcoming well-known limitations of standard CD detection, like its weak signal or its difficulties with magnetic objects [23].

For comprehensiveness, we next present a summary of concepts associated with the helicity and its optical theorem. Then, we show how general optical fields, expressed by its angular spectrum of plane waves, may be represented as a superposition of CPL components of right handed (RCP) and/or left-handed (LCP) polarization. This explicitly formulates in a quantitative manner previous descriptions of helicity of general wavefields, and permits us to introduce a class of elliptically polarized hypergeometric beams, as well as their Hermite and Laguerre derivations, which naturally appear when such representation is applied to a Gaussian angular spectrum.

We then establish how the helicity optical theorem, applied to arbitrary fields and to chiral optical beams in particular, leads to a unified generalization of the theory of dichroism. A first consequence of which is *to put forward the way of enhancing either the extinction of helicity and hence the dichroic signal, or the extinction of intensity*. Such configurations and detections are amenable to future experiments.

(a) The excitation of helicity

Quasimonochromatic fields have a time-harmonic dependence, i.e. their electric and magnetic vectors \mathcal{E} and \mathcal{B} are described in terms of their complex representations \mathbf{E} and \mathbf{B} as: $\mathcal{E}(\mathbf{r}, t) = \Re[\mathbf{E}(\mathbf{r}) \exp(-i\omega t)]$ and $\mathcal{B}(\mathbf{r}, t) = \Re[\mathbf{B}(\mathbf{r}) \exp(-i\omega t)]$, respectively. \Re denoting real part. Then, the two fundamental quantities we deal with in this work are the *helicity density*, \mathcal{H} , and the *density of flow of helicity*, \mathcal{F} , which in a non-absorbing dielectric medium of permittivity ϵ , permeability μ and refractive index $n = \sqrt{\epsilon\mu}$ are [6,16]: $\mathcal{H} = \langle \mathcal{H} \rangle = (1/2k) \sqrt{\epsilon/\mu} \Im(\mathbf{E} \cdot \mathbf{B}^*)$ and $\mathcal{F} = \langle \mathcal{F} \rangle = (c/4nk) \Im(\epsilon \mathbf{E}^* \times \mathbf{E} + (1/\mu) \mathbf{B}^* \times \mathbf{B})$. $\langle \cdot \rangle$ denoting time-average, \Im meaning imaginary part and $k = n\omega/c$. It must be recalled that for these time-harmonic fields \mathcal{F} coincides with the *spin angular momentum density* and is [4,6,15,16] k^2 times the *flow of chirality*. On the other hand, \mathcal{H} is k^2 times the *chirality*. Also, they fulfil the continuity equation [4,6,15,16]: $\mathcal{H} + \nabla \cdot \mathcal{F} = -\mathcal{D}$. Where the helicity dissipation on interaction of the fields with matter is represented by \mathcal{D} .

Let a quasi-monochromatic field, whose space-dependent complex representation is denoted as $\mathbf{E}_i, \mathbf{B}_i$, illuminate a particle which we consider magnetodielectric and bi-isotropic [24,25], dipolar in the wide sense, i.e. if for instance it is a sphere, its magnetodielectric response is characterized by its electric, magnetic and magnetoelectric polarizabilities: $\alpha_e, \alpha_m, \alpha_{em}, \alpha_{me}$,

given by the first-order Mie coefficients as $\alpha_e = i(3/2k^3)a_1$, $\alpha_m = i(3/2k^3)b_1$, $\alpha_{em} = i(3/2k^3)c_1$, $\alpha_{me} = i(3/2k^3)d_1 = -\alpha_{em}$. a_1 , b_1 and $c_1 = -d_1$ standing for the electric, magnetic and magnetoelectric first Mie coefficients, respectively [25,26]. The condition $\alpha_{em} = -\alpha_{me}$ expressing that the object is chiral. We remark that by *particle* we shall understand small objects such as atoms, molecules, material macroscopic particles or quantum dots.

The electric and magnetic dipole moments, \mathbf{p} and \mathbf{m} , induced in the particle by this incident field are

$$\mathbf{p} = \alpha_e \mathbf{E}_i + \alpha_{em} \mathbf{B}_i, \quad \mathbf{m} = \alpha_{me} \mathbf{E}_i + \alpha_m \mathbf{B}_i. \quad (1.1)$$

At any point outside this scattering object, the total field is written as $\mathbf{E}(\mathbf{r}) = \mathbf{E}_i(\mathbf{r}) + \mathbf{E}_s(\mathbf{r})$, $\mathbf{B}(\mathbf{r}) = \mathbf{B}_i(\mathbf{r}) + \mathbf{B}_s(\mathbf{r})$. The subindex s denoting the scattered, or radiated, field.

The *optical theorem* that rules the *conservation of helicity* described by the above-mentioned equation, $\mathcal{H} + \nabla \cdot \mathcal{F} = -\mathcal{P}$, is [16]

$$-\mathcal{W}_{\mathcal{H}}^a = \frac{8\pi ck^3}{3\epsilon} \Im[\mathbf{p} \cdot \mathbf{m}^*] - \frac{2\pi c}{\mu} \Re \left\{ -\frac{1}{\epsilon} \mathbf{p} \cdot \mathbf{B}_i^* + \mu \mathbf{m} \cdot \mathbf{E}_i^* \right\}. \quad (1.2)$$

On the left side of (1.2), $\mathcal{W}_{\mathcal{H}}^a$ is the rate of *dissipation* by the particle of the incident field helicity. It comes from the integration of \mathcal{P} in a volume that contains this body. On the other hand, from the Gauss divergence theorem the terms in the right side of (1.2) arise from the flow of \mathcal{F} across a surface that contains the particle [16]. The first of these terms represents the *total helicity scattered or radiated* by the object, whereas the second one constitutes the *extinction of helicity* of the incident wave on scattering. This latter extinction term $-(2\pi c/\mu)\Re\{- (1/\epsilon)\mathbf{p} \cdot \mathbf{B}_i^* + \mu \mathbf{m} \cdot \mathbf{E}_i^*\}$ should be used for determining both dissipated and radiated, or scattered, helicity by a dipolar particle in an arbitrary, homogeneous or inhomogeneous, embedding medium. To emphasize this interpretation, we recall its analogy with the well-known optical theorem for energies [27]

$$-\mathcal{W}^a = \frac{ck^4}{3n} [\epsilon^{-1} |\mathbf{p}|^2 + \mu |\mathbf{m}|^2] - \frac{\omega}{2} \Im[\mathbf{p} \cdot \mathbf{E}_i^* + \mathbf{m} \cdot \mathbf{B}_i^*]. \quad (1.3)$$

\mathcal{W}^a being the rate of energy absorption from the illuminating wave. In the right side of (1.3), the first term constitutes the total energy scattered by the dipolar object, whereas the second one represents the energy extinguished from the illuminating field, or rate of energy excitation in the scattering object.

Henceforth, we remark the analogous role played by the right-side terms in both optical theorems (1.2) and (1.3). As it is well known, $(\omega/2)\Im[\mathbf{p} \cdot \mathbf{E}^* + \mathbf{m} \cdot \mathbf{B}^*]$ has been extensively employed for characterizing dipole optical interactions [28–30]. We thus expect that progress on research of radiation–matter interactions with chiral fields will give rise to a growing use of the helicity extinction in equation (1.2): $(2\pi c/\mu)\Re\{-\epsilon^{-1}\mathbf{p} \cdot \mathbf{B}_i^* + \mu \mathbf{m} \cdot \mathbf{E}_i^*\}$. Based on this reasoning, we find it natural to introduce an *enhancement factor* $F_{\mathcal{H}}$ for the emission of helicity in analogy with the Purcell factor for a radiating electric and/or magnetic dipole: $F = 1 + (3/2k^3)\Im[\mathbf{p} \cdot \mathbf{E}^* + \mathbf{m} \cdot \mathbf{B}^*]/[\epsilon^{-1}|\mathbf{p}|^2 + \mu|\mathbf{m}|^2]$, viz.

$$F_{\mathcal{H}} = 1 + \frac{3\epsilon}{4\mu k^3} \frac{\Re\{- (1/\epsilon)\mathbf{p} \cdot \mathbf{B}_i^* + \mu \mathbf{m} \cdot \mathbf{E}_i^*\}}{\Im[\mathbf{p} \cdot \mathbf{m}^*]}. \quad (1.4)$$

In this connection, and analogously to the complex Poynting vector theorem of energy conservation (see section 6.10 of [31] and also [21,22]), the integration of the above-mentioned continuity equation for a lossy particle of volume V with constitutive parameters $\epsilon = \epsilon_R + i\epsilon_I$ and $\mu = \mu_R + i\mu_I$, in the absence of induced currents, yields (1.2) with: $\mathcal{W}_{\mathcal{H}}^a = (c^2/2n^2) \int_V dv (\epsilon_R \mu_I + \epsilon_I \mu_R) \Im[\mathbf{E} \cdot \mathbf{B}^*/\mu^*]$; which links fields in, or close to, the object with those in any other region of space; in particular in the far-zone.

2. The angular spectrum of circularly polarized plane wave components

We address the wide variety of fields propagating in a half-space $z > 0$, or $z < 0$, free from sources, represented by an angular spectrum of plane waves [32,33]. This includes optical fields. Such

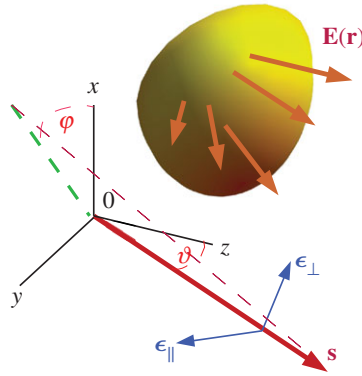


Figure 1. A field $\mathbf{E}(\mathbf{r})$, with wavefront shown by the brown-yellow surface, propagates into the half-space $z > 0$ along arbitrary directions (light-brown arrows). In the $OXYZ$ framework, the propagation vector along \mathbf{s} of each plane wave component of $\mathbf{E}(\mathbf{r})$ has polar and azimuthal angles θ and ϕ . The polarization of each of these plane waves is characterized by the orthonormal system $\{\epsilon_{\perp}, \epsilon_{\parallel}, \mathbf{s}\}$. The unit vector ϵ_{\parallel} is in the polar plane containing both \mathbf{s} and its projection (green broken line) on OXY , and points in the rotation sense of θ . On the other hand, ϵ_{\perp} is normal to this plane and points against the sense of rotation of ϕ . (Online version in colour.)

representation of either incident and scattered fields, with subindex i and s respectively, is

$$\mathbf{E}_{i,s}(\mathbf{r}) = \int_{\mathcal{D}} \mathbf{e}_{i,s}(\mathbf{s}_{\perp}) e^{ik(\mathbf{s}\cdot\mathbf{r})} d\Omega, \quad \mathbf{B}_{i,s}(\mathbf{r}) = \int_{\mathcal{D}} \mathbf{b}_{i,s}(\mathbf{s}_{\perp}) e^{ik(\mathbf{s}\cdot\mathbf{r})} d\Omega. \quad (2.1)$$

The integration being done on the contour \mathcal{D} that contains both propagating and evanescent waves [32,33]. $\mathbf{s} = (\mathbf{s}_{\perp}, s_z)$ is the unit wavevector of the plane wave component of amplitude $\mathbf{e}_{i,s}(\mathbf{s}_{\perp})$ and $\mathbf{b}_{i,s}(\mathbf{s}_{\perp})$, where $\mathbf{s}_{\perp} = (s_x, s_y, 0)$ and $s_z = \pm\sqrt{1 - |\mathbf{s}_{\perp}|^2}$ if $|\mathbf{s}_{\perp}|^2 \leq 1$ (propagating components), and $s_z = \pm i\sqrt{|\mathbf{s}_{\perp}|^2 - 1}$ if $|\mathbf{s}_{\perp}|^2 > 1$ (evanescent components). $d\Omega = \sin\theta d\theta d\phi$. $s_x = \sin\theta \cos\phi$, $s_y = \sin\theta \sin\phi$, $s_z = \cos\theta$. $0 \leq \phi \leq 2\pi$, $0 \leq \theta \leq \pi/2$ for propagating components and $\theta = \pi/2 - i\delta$, $0 < \delta \leq \infty$ for evanescent components. The $+$ or $-$ sign in s_z applies according to whether propagation is in $z > 0$ or $z < 0$, respectively. We shall assume the first case. For $z < 0$, the results are similar. In general, all plane wave components are elliptically polarized. For the incident and scattered fields one has: $\mathbf{b}_{i,s}(\mathbf{s}_{\perp}) = m\mathbf{s} \times \mathbf{e}_{i,s}(\mathbf{s}_{\perp})$, $\mathbf{e}_{i,s}(\mathbf{s}_{\perp}) \cdot \mathbf{s} = \mathbf{b}_{i,s}(\mathbf{s}_{\perp}) \cdot \mathbf{s} = 0$. The complex amplitudes of the scattered, or radiated, field angular spectrum being

$$\left. \begin{aligned} \mathbf{e}_s(\mathbf{s}_{\perp}) &= k^2 \left[\epsilon^{-1}(\mathbf{s} \times \mathbf{p}) \times \mathbf{s} - \sqrt{\frac{\mu}{\epsilon}}(\mathbf{s} \times \mathbf{m}) \right] \\ \mathbf{b}_s(\mathbf{s}_{\perp}) &= k^2 \left[\mu(\mathbf{s} \times \mathbf{m}) \times \mathbf{s} + \sqrt{\frac{\mu}{\epsilon}}(\mathbf{s} \times \mathbf{p}) \right]. \end{aligned} \right\} \quad (2.2)$$

and

For each plane wave component with wavevector $k\mathbf{s}$ of either the incident or the scattered field (2.1), we consider an orthonormal set of unit vectors (cf. figure 1) $\{\hat{\epsilon}_{\perp}, \hat{\epsilon}_{\parallel}, \mathbf{s}\}$ from which we define an helicity basis of rotating vectors: $\epsilon^{\pm}(\mathbf{s}) = (1/\sqrt{2})(\hat{\epsilon}_{\perp}(\mathbf{s}) \pm i\hat{\epsilon}_{\parallel}(\mathbf{s}))$, $\epsilon^{\pm*}(\mathbf{s}) \cdot \epsilon^{\mp}(\mathbf{s}) = 0$. Then each incident or scattered component complex amplitude is expressed as the sum of a left-handed (LCP, sign '+') and a right-handed (RCP, sign '-') circularly polarized plane wave in its corresponding framework $\{\hat{\epsilon}_{\perp}, \hat{\epsilon}_{\parallel}, \mathbf{s}\}$ according to

$$\mathbf{e}_{i,s}(\mathbf{s}_{\perp}) = e_{i,s}^{+}(\mathbf{s}_{\perp})\epsilon^{+}(\mathbf{s}) + e_{i,s}^{-}(\mathbf{s}_{\perp})\epsilon^{-}(\mathbf{s}) \quad (2.3)$$

and

$$\mathbf{b}_{i,s}(\mathbf{s}_{\perp}) = b_{i,s}^{+}(\mathbf{s}_{\perp})\epsilon^{+}(\mathbf{s}) + b_{i,s}^{-}(\mathbf{s}_{\perp})\epsilon^{-}(\mathbf{s}) = -ni[e_{i,s}^{+}(\mathbf{s}_{\perp})\epsilon^{+}(\mathbf{s}) - e_{i,s}^{-}(\mathbf{s}_{\perp})\epsilon^{-}(\mathbf{s})]. \quad (2.4)$$

With equation $\nabla \cdot \mathbf{E} = 0$ imposing according to (2.1) that $\boldsymbol{\epsilon}^\pm(\mathbf{s}) \cdot \mathbf{s} = 0$. In this representation, the helicity density of each incident or scattered plane wave component reads

$$\mathcal{H}^{i,s}(\mathbf{s}_\perp) = \left(\frac{\epsilon}{k}\right) \Im[e_{i,sx}^*(\mathbf{s}_\perp)e_{i,sy}(\mathbf{s}_\perp)] = \left(\frac{\epsilon}{2k}\right) S_3(\mathbf{s}_\perp) = \left(\frac{\epsilon}{2k}\right) [|e_{i,s}^+(\mathbf{s}_\perp)|^2 - |e_{i,s}^-(\mathbf{s}_\perp)|^2]. \quad (2.5)$$

That is, as the difference between the LCP and RCP intensities of this angular component of wavevector $k\mathbf{s}$. $S_3(\mathbf{s}_\perp)$ is the fourth Stokes parameter [27,34]. Also $|e_{i,s}(\mathbf{s}_\perp)|^2 = |e_{i,sx}(\mathbf{s}_\perp)|^2 + |e_{i,sy}(\mathbf{s}_\perp)|^2 = (8\pi/c)\sqrt{\mu/\epsilon}\langle S_{i,s}(\mathbf{s}_\perp) \rangle = 8\pi/\epsilon\langle w_{i,s}(\mathbf{s}_\perp) \rangle$. $\langle S_{i,s}(\mathbf{s}_\perp) \rangle$ and $\langle w_{i,s}(\mathbf{s}_\perp) \rangle$ representing the time-averaged Poynting vector magnitude and electromagnetic energy density, respectively: $\langle w_{i,s}(\mathbf{s}_\perp) \rangle = \langle w_{ei,s}(\mathbf{s}_\perp) \rangle + \langle w_{mi,s}(\mathbf{s}_\perp) \rangle$. $\langle w_{ei,s}(\mathbf{s}_\perp) \rangle = (\epsilon/16\pi)|\mathbf{e}_{i,s}(\mathbf{s}_\perp)|^2$, $\langle w_{mi,s}(\mathbf{s}_\perp) \rangle = (1/16\pi\mu)|\mathbf{b}_{i,s}(\mathbf{s}_\perp)|^2$.

Therefore, for the incident or the scattered field we have from (2.1), (2.3) and (2.4) the following splitting into LCP and RCP waves

$$\mathbf{E}_{i,s}(\mathbf{r}) = \mathbf{E}_{i,s}^+(\mathbf{r}) + \mathbf{E}_{i,s}^-(\mathbf{r}); \quad \mathbf{B}_{i,s}(\mathbf{r}) = \mathbf{B}_{i,s}^+(\mathbf{r}) + \mathbf{B}_{i,s}^-(\mathbf{r}) = -ni[\mathbf{E}_{i,s}^+(\mathbf{r}) - \mathbf{E}_{i,s}^-(\mathbf{r})] \quad (2.6)$$

and

$$\mathbf{E}_{i,s}^\pm(\mathbf{r}) = \int_{\mathcal{D}} e_{i,s}^\pm(\mathbf{s}_\perp)\boldsymbol{\epsilon}^\pm(\mathbf{s})e^{i\mathbf{k}(\mathbf{s}\cdot\mathbf{r})}d\Omega. \quad (2.7)$$

Assuming the particle chiral, $\alpha_{em} = -\alpha_{me}$, and introducing equations (2.7) into (1.1) we write

$$\mathbf{p}(\mathbf{r}) = \mathbf{p}_+(\mathbf{r}) + \mathbf{p}_-(\mathbf{r}); \quad \mathbf{m}(\mathbf{r}) = \mathbf{m}_+(\mathbf{r}) + \mathbf{m}_-(\mathbf{r}). \quad (2.8)$$

With

$$\mathbf{p}_\pm(\mathbf{r}) = (\alpha_e \pm ni\alpha_{me})\mathbf{E}_i^\pm(\mathbf{r}). \quad \mathbf{m}_\pm(\mathbf{r}) = (\alpha_{me} \mp ni\alpha_m)\mathbf{E}_i^\pm(\mathbf{r}). \quad (2.9)$$

And substituting (2.1) into (2.9), we see that $\mathbf{p}_\pm(\mathbf{r})$ and $\mathbf{m}_\pm(\mathbf{r})$ also admit an angular spectrum representation like (2.1), their respective angular spectra being

$$\hat{\mathbf{p}}_\pm(\mathbf{s}_\perp) = (\alpha_e \pm ni\alpha_{me})e_i^\pm(\mathbf{s}_\perp)\boldsymbol{\epsilon}^\pm(\mathbf{s}); \quad \hat{\mathbf{m}}_\pm(\mathbf{s}_\perp) = (\alpha_{me} \mp ni\alpha_m)e_i^\pm(\mathbf{s}_\perp)\boldsymbol{\epsilon}^\pm(\mathbf{s}). \quad (2.10)$$

So that from (2.10), (2.8) and (2.2), we obtain for the scattered field angular spectrum

$$\left. \begin{aligned} a_s^\pm(\mathbf{s}_\perp) &= k^2 \left[\frac{\alpha_e \pm ni\alpha_{me}}{\epsilon} \pm i\sqrt{\frac{\mu}{\epsilon}}(\alpha_{me} \mp ni\alpha_m) \right] e_i^\pm(\mathbf{s}_\perp) \\ b_s^\pm(\mathbf{s}_\perp) &= k^2 \left[\mp i\sqrt{\frac{\mu}{\epsilon}}(\alpha_e \pm ni\alpha_{me}) + \mu(\alpha_{me} \mp ni\alpha_m) \right] e_i^\pm(\mathbf{s}_\perp). \end{aligned} \right\} \quad (2.11)$$

We obtain the helicity densities $\mathcal{H}_{i,s}$ for either the incident or scattered fields by introducing (2.3) and (2.4) into (2.1), and inserting the result into the definition introduced in §1a: $\mathcal{H} = \langle \mathcal{H} \rangle = (1/2k)\sqrt{\epsilon/\mu}\Im(\mathbf{E} \cdot \mathbf{B}^*)$. Then since after taking imaginary parts the cross-terms containing the integrand factors $nie_{i,s}^+(\mathbf{s}_\perp)e_{i,s}^{-*}(\mathbf{s}'_\perp)\boldsymbol{\epsilon}^+(\mathbf{s}) \cdot \boldsymbol{\epsilon}^{-*}(\mathbf{s}')$ and $-nie_{i,s}^{+*}(\mathbf{s}_\perp)e_{i,s}^-(\mathbf{s}'_\perp)\boldsymbol{\epsilon}^{+*}(\mathbf{s}) \cdot \boldsymbol{\epsilon}^-(\mathbf{s}')$ cancel each other, we finally get

$$\mathcal{H}_{i,s}(\mathbf{r}) = \frac{\epsilon}{2k} [|\mathbf{E}_{i,s}^+(\mathbf{r})|^2 - |\mathbf{E}_{i,s}^-(\mathbf{r})|^2]. \quad (2.12)$$

Equation (2.12) introduced in the optical theorem for the helicity, (1.2), accounts for all chirality effects due to the interaction of waves with dipolar particles, both in the propagating region (real s_i^z) of the angular spectrum, as in the evanescent domain (imaginary s_i^z). The latter applies in particular for the interaction of plasmon polaritons with particles on metallic surfaces.

Expressions (2.12) are of particular importance in the far zone $kr \rightarrow \infty$, where [32,33]

$$\mathbf{E}_{i,s}^\pm(r\hat{\mathbf{s}}) \approx -(2\pi i/k)e_{i,s}^\pm(\hat{\mathbf{s}}_\perp)\boldsymbol{\epsilon}^\pm(\hat{\mathbf{s}})\exp(ikr)/r. \quad (2.13)$$

$e_s^\pm(\hat{\mathbf{s}}_\perp)\boldsymbol{\epsilon}^\pm(\hat{\mathbf{s}})$ plays the role of the CPL complex amplitude for a radiated, or scattered, field, and $\hat{\mathbf{s}} = \mathbf{r}/r$ now belongs to the domain of propagating components only. Dropping the sub-indices

i, s to simplify notation, equations (2.12) and (2.13) lead for either the incident or the scattered field to

$$\mathcal{H}_{\text{ff}}(r\hat{s}) = \frac{2\pi^2\epsilon}{k^3r^2} [|e^+(\hat{s}_\perp)|^2 - |e^-(\hat{s}_\perp)|^2]. \quad (2.14)$$

And their density of flow of helicity is $\mathcal{F}_{\text{ff}}(r\hat{s}) = (c/n)\mathcal{H}_{\text{ff}}(\mathbf{r})\hat{s}$, which in agreement with the conservation of helicity, expresses on integration in a large sphere surrounding the scatterer that the outgoing helicity flow of the field across any plane $z = \text{constant}$, or closed surface, outside the scattering volume, which equals the flow of helicity across any sphere at infinity, is equal to c/n times the total helicity enclosed by that sphere: $\int_{z=0} \mathcal{F}(\mathbf{r}) \cdot \hat{z} \, dx \, dy = \int_{r \rightarrow \infty} \mathcal{F}_{\text{ff}}(r\hat{s}) \cdot \mathbf{r} \, r^2 \, d\Omega$. Where now the solid angle Ω spans on the whole sphere of real angles only. Taking into account (2.12), and in analogy with the flow of energy [32,33], one sees that the evanescent components do not contribute to the flux of helicity across the plane $z = 0$ in the half-space $z \geq 0$.

(a) A particular case: incident elliptically polarized plane wave

The significance of the optical theorem (1.2) for the helicity—or chirality—of wavefields is illustrated considering one of the simplest and most employed configurations: one elliptically polarized incident plane wave impinging on a dipolar particle with wavevector $k\mathbf{s}_i$ along OZ. According to (2.3) and (2.4) the fields are $\mathbf{e}_i = (e_{ix}, e_{iy}, 0) = e_i^+ \boldsymbol{\epsilon}^+ + e_i^- \boldsymbol{\epsilon}^-$. $\mathbf{b}_i = (b_{ix}, b_{iy}, 0) = n(-e_{iy}, e_{ix}, 0) = b_i^+ \boldsymbol{\epsilon}^+ + b_i^- \boldsymbol{\epsilon}^- = -ni(e_i^+ \boldsymbol{\epsilon}^+ - e_i^- \boldsymbol{\epsilon}^-)$.

So that the incident helicity density reads

$$\mathcal{H}^i = \left(\frac{\epsilon}{k}\right) \Im[e_{ix}^* e_{iy}] = \left(\frac{\epsilon}{2k}\right) S_3 = \left(\frac{\epsilon}{2k}\right) [|e_i^+|^2 - |e_i^-|^2]. \quad (2.15)$$

Also, according to (2.8) and (2.9): $\mathbf{p} = p_+ \boldsymbol{\epsilon}^+ + p_- \boldsymbol{\epsilon}^-$, $p_\pm = (\alpha_e \mp n\alpha_{\text{em}})e_i^\pm$; $\mathbf{m} = m_+ \boldsymbol{\epsilon}^+ + m_- \boldsymbol{\epsilon}^-$, $m_\pm = (\alpha_{\text{me}} \mp n\alpha_{\text{m}})e_i^\pm$.

On introducing, these dipole moments and fields into the optical theorems of helicity (1.2) and energy (1.3), they yield for the rate of helicity and energy extinction

$$\Im\{(p_+ + inm_+)e_i^{+*} - (p_- - inm_-)e_i^{-*}\} = \frac{4k^3n}{3\epsilon} \Im\{p_+m_+^* + p_-m_-^*\} + \mathcal{W}_{\mathcal{A}}^a \quad (2.16)$$

and

$$\Im\{(p_+ + inm_+)e_i^{+*} + (p_- - inm_-)e_i^{-*}\} = \frac{2k^3}{3\epsilon} \{|p_+|^2 + |p_-|^2 + n^2(|m_+|^2 + |m_-|^2)\} + \mathcal{W}^a, \quad (2.17)$$

respectively. Equation (2.16) is identical to the CD law, usually mechanoquantically formulating molecular absorption and fluorescence effects [18]. However, equations (2.16) and (2.17), obtained from classical electrodynamics, include the rate of helicity and energy dissipation both by absorption and scattering (or diffraction), and generalize the CD theory to any wide sense dipolar ‘particle’ or structure.

In other words, the CD phenomenon is not only characterized by the operation of taking the difference of energy absorption and emission $\Im[\mathbf{p} \cdot \mathbf{E}_i^* + \mathbf{m} \cdot \mathbf{B}_i^*]$ by chiral molecules as they are separately illuminated by RCP and LCP waves; i.e. as this absorbed energy is $\Im\{(p_+ + inm_+)e_i^{+*}\}$ and $\Im\{(p_- - inm_-)e_i^{-*}\}$, respectively, as usually considered so far [17–19]. But CD is also, and fundamentally, one of the physical manifestations of the conservation law of electromagnetic helicity—or chirality—and is represented by the left-side extinction term of (2.16), $\Re[-(1/\epsilon)\mathbf{p} \cdot \mathbf{B}_i^* + \mu\mathbf{m} \cdot \mathbf{E}_i^*] = \Im\{(p_+ + inm_+)e_i^{+*} - (p_- - inm_-)e_i^{-*}\}$ of the helicity optical theorem (1.2); being involved in any scattering and/or absorption process of LCP and RCP electromagnetic waves, thus characterizing the rate of extinction helicity, or chirality. In addition, as shown by equation (2.10) and (2.16), CD arises not only due the chirality of the scattering object, represented by α_{me} , but also and primarily by the mere induction of their electric and/or magnetic dipoles.

Hence it is not surprising that the ratio of the extinction of incident field helicity (2.16) and energy (2.17) is identical to the well-known *dissymmetry factor* of CD [4,17,19]. Moreover, adding and subtracting (2.16) and (2.17) yield the energy excitation by extinction of the respective LCP

or RCP component of the incident elliptically polarized light according to the dipole handedness p_{\pm} and/or m_{\pm} :

$$\Im\{(p_{\pm} \pm inm_{\pm})e_i^{\pm*}\} = \frac{k^3}{3\epsilon}\{|p_{+} \pm inm_{+}|^2 + |p_{-} \pm inm_{-}|^2\} + \frac{1}{2}(\mathcal{W}^a \pm \mathcal{W}_{\mathcal{H}}^a). \quad (2.18)$$

(b) The special case of an incident circularly polarized plane wave

Let the field incident on the particle be just one CPL component, either LCP or RCP, then $e_i^{\pm} = e\epsilon^{\pm}$ and $\mathbf{p} = p_{\pm}\epsilon^{\pm}$, $\mathbf{m} = m_{\pm}\epsilon^{\pm}$, and (2.18) lead to

$$\Im\{(p_{\pm} \pm inm_{\pm})e_i^{\pm*}\} = \frac{k^3}{3\epsilon}\{|p_{\pm}|^2 + n^2|m_{\pm}|^2 \pm 2n\Im\{p_{\pm}m_{\pm}^*\}\} + \frac{1}{2}(\mathcal{W}^a \pm \mathcal{W}_{\mathcal{H}}^a) \quad (2.19)$$

and

$$\frac{k^3}{3\epsilon}|p_{\pm} \mp inm_{\pm}|^2 + \frac{1}{2}(\mathcal{W}^a \mp \mathcal{W}_{\mathcal{H}}^a) = 0. \quad (2.20)$$

From which we obtain

$$2n\Im\{p_{\pm}m_{\pm}^*\} = \pm[|p_{\pm}|^2 + n^2|m_{\pm}|^2 + \frac{1}{2}(\mathcal{W}^a \mp \mathcal{W}_{\mathcal{H}}^a)]. \quad (2.21)$$

Thus, apart from a constant factor, for CPL incidence the scattered helicity equals in modulus the scattered energy plus the rates of dissipation of helicity and energy, and has a sign that depends on the handedness of the incident light. Of course (2.19)–(2.21) are consistent, as they should, with equations (2.16) and (2.17), which for CPL become

$$\Im\{(p_{\pm} \pm inm_{\pm})e_i^{\pm*}\} = \pm \frac{4k^3n}{3\epsilon}\Im\{p_{\pm}m_{\pm}^*\} \pm \mathcal{W}_{\mathcal{H}}^a = \frac{2k^3}{3\epsilon}\{|p_{\pm}|^2 + n^2|m_{\pm}|^2\} + \mathcal{W}^a. \quad (2.22)$$

A comparison of (2.22) with (2.16) and (2.17) shows that the excitation of the particle by both the LCP and RCP components of an elliptically polarized plane wave is equivalent to performing two observations separately: one with an LCP plane wave only, and another one with only RCP (each of which is ruled by (2.22) with the corresponding sign), and then subtracting or adding the respective excitations given by the left sides of (2.22). This operation reproduces the left side of (2.16) and (2.17), respectively. In other words, equations (2.16) and (2.17) show that *the LCP and RCP components of an incident elliptically polarized plane wave do not interfere and, hence, interact independently of each other with the particle.*

As regards equation (2.20), because often in molecular spectroscopy $|m_{\pm}| \ll |p_{\pm}|$, the value of \mathcal{W}^a and/or $\mathcal{W}_{\mathcal{H}}^a$ contributes to that of $|p_{\pm}|$. Nonetheless, equation (2.20) is also compatible with the electric and magnetic dipoles excited by CPL light, and the absorption rates, fulfilling

$$p_{\pm} = \pm inm_{\pm} \Leftrightarrow \mathcal{W}_{\mathcal{H}}^a = \pm \mathcal{W}^a. \quad (2.23)$$

Hence *this is a sufficient condition for an electric–magnetic dipole to emit chiral light.* Particularly remarkable is this latter case is when the dissipation rates of helicity and energy either cancel each other, or the particle introduces no energy or helicity losses, $\mathcal{W}^a = \mathcal{W}_{\mathcal{H}}^a = 0$, so that all energy and helicity extinguished from the incident field are re-radiated by elastic scattering. As seen from (2.20), in that case $2n\Im\{p_{\pm}m_{\pm}^*\} = \pm[|p_{\pm}|^2 + n^2(|m_{\pm}|^2)]$, which states that then the optical theorems for helicity, equation (2.16), and energy, equation (2.17), are equivalent, and the scattered helicity is proportional to the scattered intensity and has a sign that depends on the handedness of the incident light, whereas the density of helicity flow (spin) is proportional to that of energy flow (Poynting vector). Thus in such a situation the optical theorems for helicity (1.2) and energy (1.3) are equivalent (see also [6,16]).

Equation (2.23) also has some important consequences.

- *The far-zone scattered field is circularly polarized.* $\mathbf{b}^{\pm}(\mathbf{s}_{\perp}) = \mp n\mathbf{ie}^{\pm}(\mathbf{s}_{\perp})$ (cf. equations (2.2)). This circular polarization holds with respect to the Cartesian system of orthogonal axes defined by the unit vectors: $(\epsilon_{\perp}, \epsilon_{\parallel}, \mathbf{s})$ (figure 1). ϵ_{\perp} and ϵ_{\parallel} being respectively

perpendicular and parallel to the polar plane (which now becomes the scattering plane) delimited by \mathbf{s} and its projection on OXY ; i.e. $\mathbf{e}^{\pm}(\mathbf{s}_{\perp}) = (\mathbf{e}(\mathbf{s}_{\perp}) \cdot \boldsymbol{\epsilon}_{\perp})(\boldsymbol{\epsilon}_{\perp} + \pm i\boldsymbol{\epsilon}_{\parallel} + 0\mathbf{s})$ and $\mathbf{b}^{\pm}(\mathbf{s}_{\perp}) = (n\mathbf{e}(\mathbf{s}_{\perp}) \cdot \boldsymbol{\epsilon}_{\perp})(\mp i\boldsymbol{\epsilon}_{\perp} + \boldsymbol{\epsilon}_{\parallel} + 0\mathbf{s})$.

From the above it should also be noticed that *it is the handedness of the dipole moments, and not necessarily the chirality α_{me} , the relevant characteristic for these CD effects*. Besides, this CPL property of the scattered field is just a consequence of the optical theorems of energy and helicity, and does not presuppose in the particle neither chirality, $\alpha_{em} = -\alpha_{me}$, nor duality, $\epsilon^{-1}\alpha_e = \mu\alpha_m$ [16]. Although the combination of both theorems imposes [16] that the existence of one these two last properties of the particle polarizabilities implies the other.

— In the near field zone, the scattered wave in the basis $(\boldsymbol{\epsilon}_{\perp}, \boldsymbol{\epsilon}_{\parallel}, \mathbf{s})$ has

$$\left. \begin{aligned} \mathbf{E}_{nf}(\mathbf{r}) &= \frac{1}{\epsilon r^3} [3\mathbf{s}(\mathbf{s} \cdot \mathbf{p}) - \mathbf{p}] = -\frac{p_{\pm}}{\epsilon r^3} e^{\pm i\phi} [\pm i\boldsymbol{\epsilon}_{\perp} + \cos\theta\boldsymbol{\epsilon}_{\parallel} - 2\sin\theta\mathbf{s}], \\ \text{and} \quad \mathbf{B}_{nf}(\mathbf{r}) &= \frac{\mu}{r^3} [3\mathbf{s}(\mathbf{s} \cdot \mathbf{m}) - \mathbf{m}] = -\frac{\mu m_{\pm}}{r^3} e^{\pm i\phi} [\pm i\boldsymbol{\epsilon}_{\perp} + \cos\theta\boldsymbol{\epsilon}_{\parallel} - 2\sin\theta\mathbf{s}]. \end{aligned} \right\} \quad (2.24)$$

Thus, this field *being CPL* at points \mathbf{r} along the polar axis OZ ($\theta = 0$, or $\theta = \pi$).

3. Excitation of helicity and energy with general optical fields: the role of angular spectra with right-circular and left-circular polarization

Returning to equations (2.6)–(2.10) for general optical fields, we have from the optical theorem for the helicity (1.2) the following expression for its extinction from the incident field on scattering by the particle-induced dipole:

$$\begin{aligned} & \Im\{[\mathbf{p}_{+}(\mathbf{r}) + in\mathbf{m}_{+}(\mathbf{r})] \cdot \mathbf{E}_i^{+*}(\mathbf{r}) - [\mathbf{p}_{-}(\mathbf{r}) - in\mathbf{m}_{-}(\mathbf{r})] \cdot \mathbf{E}_i^{-*}(\mathbf{r})\} + 2\Re\{\alpha_e - n^2\alpha_m\} \\ & \times \Im\{\mathbf{E}_i^{-}(\mathbf{r}) \cdot \mathbf{E}_i^{+*}(\mathbf{r})\} = \frac{4k^3n}{3\epsilon} \Im\{\mathbf{p}_{+}(\mathbf{r}) \cdot \mathbf{m}_{+}^{*}(\mathbf{r}) + \mathbf{p}_{-}(\mathbf{r}) \cdot \mathbf{m}_{-}^{*}(\mathbf{r})\} \\ & + \text{CD}(\mathbf{r}) + \frac{n}{2\pi c} \mathcal{W}_{\mathcal{H}}^a. \end{aligned} \quad (3.1)$$

While the extinction of incident energy is according to the standard optical theorem (1.3)

$$\begin{aligned} & \Im\{[\mathbf{p}_{+}(\mathbf{r}) + in\mathbf{m}_{+}(\mathbf{r})] \cdot \mathbf{E}_i^{+*}(\mathbf{r}) + [\mathbf{p}_{-}(\mathbf{r}) - in\mathbf{m}_{-}(\mathbf{r})] \cdot \mathbf{E}_i^{-*}(\mathbf{r})\} + 2\Im\{\alpha_e - n^2\alpha_m\} \\ & \times \Re\{\mathbf{E}_i^{-}(\mathbf{r}) \cdot \mathbf{E}_i^{+*}(\mathbf{r})\} = \frac{2k^3}{3\epsilon} \{|\mathbf{p}_{+}(\mathbf{r})|^2 + |\mathbf{p}_{-}(\mathbf{r})|^2 + n^2[|\mathbf{m}_{+}(\mathbf{r})|^2 + |\mathbf{m}_{-}(\mathbf{r})|^2]\} \\ & + \text{CE}(\mathbf{r}) + \frac{2}{\omega} \mathcal{W}^a. \end{aligned} \quad (3.2)$$

The terms $\text{CD}(\mathbf{r})$ and $\text{CE}(\mathbf{r})$ are

$$\text{CD}(\mathbf{r}) = \frac{8k^3n}{3\epsilon} [\Im\{(\alpha_e - n^2\alpha_m)\alpha_{me}^{*}\} \Re\{\mathbf{E}_i^{-}(\mathbf{r}) \cdot \mathbf{E}_i^{+*}(\mathbf{r})\} - n\Im\{\alpha_e\alpha_m^{*}\} \Im\{\mathbf{E}_i^{-}(\mathbf{r}) \cdot \mathbf{E}_i^{+*}(\mathbf{r})\}] \quad (3.3)$$

and

$$\text{CE}(\mathbf{r}) = \frac{4k^3}{3\epsilon} [|\alpha_e|^2 - n^4|\alpha_m|^2] \Re\{\mathbf{E}_i^{-}(\mathbf{r}) \cdot \mathbf{E}_i^{+*}(\mathbf{r})\} + 2n\Re\{(\alpha_e - n^2\alpha_m)\alpha_{me}^{*}\} \Im\{\mathbf{E}_i^{-}(\mathbf{r}) \cdot \mathbf{E}_i^{+*}(\mathbf{r})\}. \quad (3.4)$$

In these equations, \mathbf{r} denotes the position vector of the centre of the particle immersed in the illuminating field. Now, in contrast with the scattering of an incident elliptically polarized plane wave discussed above, the scattered helicity and energy convey interference between \mathbf{E}_i^{-} and \mathbf{E}_i^{+} .

Note that by virtue of the asymptotic expression (2.13), in the far-zone $\text{CD}(\hat{\mathbf{r}}\hat{\mathbf{s}}) = \text{CE}(\hat{\mathbf{r}}\hat{\mathbf{s}}) = 0$ as $\boldsymbol{\epsilon}^{\pm*}(\hat{\mathbf{s}}) \cdot \boldsymbol{\epsilon}^{\mp}(\hat{\mathbf{s}}) = 0$. It is also interesting to observe from (3.1)–(3.4) that if the particle is dual,

$\alpha_e = n^2 \alpha_m$, the terms of interference between \mathbf{E}^+ and \mathbf{E}^- are zero and so are CD(\mathbf{r}) and CE(\mathbf{r}) for any \mathbf{r} . Then (3.1) and (3.2) reduce to equations similar to (2.16) and (2.17).

However, the important point is that now the appearance of the interference factor $[\mathbf{E}_i^-(\mathbf{r}) \cdot \mathbf{E}_i^{+*}(\mathbf{r})]$ in (3.1) and (3.2) allows one to choose the incident field such that either $\Im[\mathbf{E}_i^- \cdot \mathbf{E}_i^{+*}]$ or $\Re[\mathbf{E}_i^- \cdot \mathbf{E}_i^{+*}]$ is zero, or small, for the extinction rates of helicity (3.1) and of intensity (3.2), respectively. We thus shall analyse the consequences of $2\Re\{\alpha_e - n^2 \alpha_m\} \Im\{\mathbf{E}_i^- \cdot \mathbf{E}_i^{+*}\}$ or $2\Im\{\alpha_e - n^2 \alpha_m\} \Re\{\mathbf{E}_i^- \cdot \mathbf{E}_i^{+*}\}$ being non-zero in the left sides of (3.1) and (3.2), respectively, as a consequence of the choice of illumination on the particle.

Using (2.9) the left sides of (3.1) and (3.2) are in terms of the polarizabilities and fields

$$\begin{aligned} & \Im\{[\mathbf{p}_+(\mathbf{r}) + i\mathbf{m}\mathbf{m}_+(\mathbf{r})] \cdot \mathbf{E}_i^{+*}(\mathbf{r}) \pm [\mathbf{p}_-(\mathbf{r}) - i\mathbf{m}\mathbf{m}_-(\mathbf{r})] \cdot \mathbf{E}_i^{-*}(\mathbf{r})\} \\ &= \Im\{\alpha_e + n^2 \alpha_m\}(|\mathbf{E}_i^+(\mathbf{r})|^2 \mp |\mathbf{E}_i^-(\mathbf{r})|^2) + 2n\Re\{\alpha_{me}\}(|\mathbf{E}_i^+(\mathbf{r})|^2 \pm |\mathbf{E}_i^-(\mathbf{r})|^2). \end{aligned} \quad (3.5)$$

By means of (3.5) we now address the rate of extinction of helicity $\mathcal{W}_{\mathcal{H}}^s$ (cf. equation (17) in [16]) and energy \mathcal{W}^s in the particle, given by the left sides of (3.1) and (3.2), as functions of the polarizabilities

$$\begin{aligned} \frac{\mu}{2\pi c} \mathcal{W}_{\mathcal{H}}^s &\equiv \Im\{[\mathbf{p}_+(\mathbf{r}) + i\mathbf{m}\mathbf{m}_+(\mathbf{r})] \cdot \mathbf{E}_i^{+*}(\mathbf{r}) - [\mathbf{p}_-(\mathbf{r}) - i\mathbf{m}\mathbf{m}_-(\mathbf{r})] \cdot \mathbf{E}_i^{-*}(\mathbf{r})\} \\ &+ 2\Re\{\alpha_e - n^2 \alpha_m\} \Im\{\mathbf{E}_i^-(\mathbf{r}) \cdot \mathbf{E}_i^{+*}(\mathbf{r})\} = \Im\{\alpha_e + n^2 \alpha_m\}(|\mathbf{E}_i^+(\mathbf{r})|^2 - |\mathbf{E}_i^-(\mathbf{r})|^2) \\ &+ 2n\Re\{\alpha_{me}\}(|\mathbf{E}_i^+(\mathbf{r})|^2 + |\mathbf{E}_i^-(\mathbf{r})|^2) + 2\Re\{\alpha_e - n^2 \alpha_m\} \Im\{\mathbf{E}_i^-(\mathbf{r}) \cdot \mathbf{E}_i^{+*}(\mathbf{r})\}. \end{aligned} \quad (3.6)$$

and

$$\begin{aligned} \frac{2}{\omega} \mathcal{W}^s &\equiv \Im\{[\mathbf{p}_+(\mathbf{r}) + i\mathbf{m}\mathbf{m}_+(\mathbf{r})] \cdot \mathbf{E}_i^{+*}(\mathbf{r}) + [\mathbf{p}_-(\mathbf{r}) - i\mathbf{m}\mathbf{m}_-(\mathbf{r})] \cdot \mathbf{E}_i^{-*}(\mathbf{r})\} \\ &+ 2\Im\{\alpha_e - n^2 \alpha_m\} \Re\{\mathbf{E}_i^-(\mathbf{r}) \cdot \mathbf{E}_i^{+*}(\mathbf{r})\} = \Im\{\alpha_e + n^2 \alpha_m\}(|\mathbf{E}_i^+(\mathbf{r})|^2 + |\mathbf{E}_i^-(\mathbf{r})|^2) \\ &+ 2n\Re\{\alpha_{me}\}(|\mathbf{E}_i^+(\mathbf{r})|^2 - |\mathbf{E}_i^-(\mathbf{r})|^2) + 2\Im\{\alpha_e - n^2 \alpha_m\} \Re\{\mathbf{E}_i^-(\mathbf{r}) \cdot \mathbf{E}_i^{+*}(\mathbf{r})\}. \end{aligned} \quad (3.7)$$

Note that $\mathcal{W}_{\mathcal{H}}^s \neq 0$ even if $\alpha_{me} = 0$ and $|\mathbf{E}_i^+(\mathbf{r})|^2 = |\mathbf{E}_i^-(\mathbf{r})|^2$. It should be remarked that in the particular case of incident CPL plane waves, or CPL beams without longitudinal component, one has (choosing propagation along e.g. OZ): $\mathbf{E}_i^+ = E_i^+ \boldsymbol{\epsilon}^+$, $\mathbf{E}_i^- = E_i^- \boldsymbol{\epsilon}^-$; and as $\Re\{\mathbf{E}_i^- \cdot \mathbf{E}_i^{+*}\} = \Im\{\mathbf{E}_i^- \cdot \mathbf{E}_i^{+*}\} = 0$, equation (3.1) becomes (2.16) and equation (3.2) reduces to (2.17). Hence, in this case \mathbf{E}_i^+ and \mathbf{E}_i^- do not interfere, and when $|\mathbf{E}_i^+| = |\mathbf{E}_i^-| = |\mathbf{E}_i|$ equations (3.6) and (3.7) are similar to those of standard circular dichroism which our formulation shows that yields the rate of helicity extinction, first with an incident LCP wave, and then with one being RCP, both of the same amplitude. In such a situation, (3.6) and (3.7) become respectively proportional to the well-known numerator, $4n\alpha_{me}^R |\mathbf{E}_i(\mathbf{r})|^2$ and denominator, $2(\alpha_e^I + n^2 \alpha_m^I) |\mathbf{E}_i(\mathbf{r})|^2$ of the CD *dissymmetry factor* [4,23]. (The superscripts R and I denoting real and imaginary part.)

However, our general equations (3.6) and (3.7) cover many other configurations (in particular those so-called superchiral fields [4], which is known, however, to be limited to molecules with $\alpha_m \simeq 0$ [23]). We next show the broader scope of (3.6) and (3.7) with chiral optical beams possessing a longitudinal component, which as we shall show, plays a key role. We will see that according to whether one chooses such illuminating beams yielding either $\Re\{\mathbf{E}_i^- \cdot \mathbf{E}_i^{+*}\} = 0$ or $\Im\{\mathbf{E}_i^- \cdot \mathbf{E}_i^{+*}\} = 0$ one respectively enhances the extinction rate of helicity (3.6) versus that of energy (3.7) (and thus the ratio between them) or vice versa. Note that because out of resonance the real part of the polarizabilities are usually greater than the imaginary parts, the last term of (3.6) may be larger than that of (3.7). Hence, one may produce bigger enhancement in $\mathcal{W}_{\mathcal{H}}^s$ than in \mathcal{W}^s with those choices of \Re and \Im of $\mathbf{E}_i^- \cdot \mathbf{E}_i^{+*}$.

4. Optical beams whose angular spectrum representation contains left-circular and right-circular plane waves

In the paraxial approximation $\partial_z \simeq ik_z$, so that the equation $\nabla \cdot \mathbf{E} = 0$ implies that $E_z = (i/k)\nabla_{\perp} \cdot \mathbf{E}_{\perp}$ [35]; (\perp denotes transversal, i.e. XY component). The electric vector of an optical beam is then written in terms of its angular spectrum as [32,33]

$$\mathbf{E}(\mathbf{r}) = e^{ikz} \int_{-\infty}^{\infty} \mathbf{e}(\mathbf{s}_{\perp}) e^{i\mathbf{k}\mathbf{s}_{\perp} \cdot \mathbf{R}} e^{-ikz \frac{|\mathbf{s}_{\perp}|^2}{2}} d^2\mathbf{s}_{\perp}. \quad (4.1)$$

Having denoted $\mathbf{r} = (\mathbf{R}, z)$, $\mathbf{R} = (x, y, 0)$, $\mathbf{s} = (\mathbf{s}_{\perp}, s_z)$, $\mathbf{s}_{\perp} = (s_x, s_y, 0)$.

We shall consider the Gaussian beam, i.e. the one from which other fields, like Hermite and Laguerre–Gaussian beams, are generated [36].

We write for (4.1) the decomposition (2.3) of each component into LCP and RCP waves by expressing the Gaussian angular spectrum [32,33] as $\mathbf{e}(\mathbf{s}_{\perp}) = (k^2 W_0^2 / 4\pi) \exp[-k^2 W_0^2 |\mathbf{s}_{\perp}|^2 / 4] [e_0^+ \boldsymbol{\epsilon}^+(\mathbf{s}) + e_0^- \boldsymbol{\epsilon}^-(\mathbf{s})]$. e_0^+ and e_0^- being complex constants, and W_0 standing for the beam waist at $z = 0$. Then, we express the beam as

$$\mathbf{E}(\mathbf{r}) = \frac{(kW_0)^2}{4\pi} e^{ikz} \int_{-\infty}^{\infty} e^{[-k^2 W_0^2 |\mathbf{s}_{\perp}|^2 / 4]} e^{i\mathbf{k}\mathbf{s}_{\perp} \cdot \mathbf{R}} e^{-ikz \frac{|\mathbf{s}_{\perp}|^2}{2}} [e_0^+ \boldsymbol{\epsilon}^+(\mathbf{s}) + e_0^- \boldsymbol{\epsilon}^-(\mathbf{s})] d^2\mathbf{s}_{\perp}. \quad (4.2)$$

Recalling that $\boldsymbol{\epsilon}^{\pm}(\mathbf{s}) = (1/\sqrt{2})(\hat{\boldsymbol{\epsilon}}_{\perp}(\mathbf{s}), \pm i\hat{\boldsymbol{\epsilon}}_{\parallel}(\mathbf{s}), 0)$, and writing in the Cartesian basis $\hat{\mathbf{x}}, \hat{\mathbf{y}}, \hat{\mathbf{z}}$ (figure 1): $\hat{\boldsymbol{\epsilon}}_{\perp}(\mathbf{s}) = (\sin \phi, \cos \phi, 0)$, $\hat{\boldsymbol{\epsilon}}_{\parallel}(\mathbf{s}) = (\cos \theta \cos \phi, \cos \theta \sin \phi, -\sin \theta)$, $\mathbf{s} = (\sin \theta \cos \phi, \sin \theta \sin \phi, \cos \theta)$, $d^2\mathbf{s}_{\perp} = d\Omega = \sin \theta \cos \theta d\theta d\phi$. $0 \leq \theta \leq \pi$, $0 \leq \phi \leq 2\pi$.

Performing the ϕ and θ integrals we obtain (see integrals 3.937.2 and 6.631.1 of [37]) after making $\cos \theta \simeq 1$ in all factors of the integrand but not in the exponentials as involved in the paraxial approximation, and writing $x + iy = R \exp(i\Phi)$, Φ being the azimuthal angle, we derive

$$\begin{aligned} \mathbf{E}(\mathbf{r}) = & \frac{W_0^2}{4\sqrt{\pi}\sigma^3} e^{ikz} \left\{ \frac{R}{2} {}_1F_1 \left(\frac{3}{2}; 2; -\frac{R^2}{2\sigma^2} \right) [-e_0^+ \exp(-i\Phi)(\hat{\mathbf{x}} + i\hat{\mathbf{y}}) + e_0^- \exp(i\Phi)(\hat{\mathbf{x}} - i\hat{\mathbf{y}})] \right. \\ & \left. + \frac{i}{k} (e_0^+ - e_0^-) {}_1F_1 \left(\frac{3}{2}; 1; -\frac{R^2}{2\sigma^2} \right) \hat{\mathbf{z}} \right\}. \end{aligned} \quad (4.3)$$

${}_1F_1$ is Kummer's confluent hypergeometric function [38]. $\sigma^2 = W_0^2/2 + iz/k$. Equation (4.3) represents a hypergeometric beam which, containing LCP and RCP plane waves, differs from some previously put forward [39]. A generalization of this beam to arbitrary index m with vortices $\exp(\pm im\Phi)$ and topological charge m is made by including a factor $\exp(-im\phi)$ in $\mathbf{e}(\mathbf{s}_{\perp})$. Note from (4.3) that due to the paraxial approximation the transversal XY -component of \mathbf{E} is the sum of two fields (cf. equation (2.7)): one, \mathbf{E}^+ , is LCP and has a complex amplitude proportional to $-e_0^+$; the other, \mathbf{E}^- , is RCP and its amplitude factors e_0^- . These two CPL beams also have a longitudinal component E_z , proportional to $(i/k)e_0^+$ and $-(i/k)e_0^-$, respectively, as shown by the last term of (4.3). Next, we see the relevance of this longitudinal component to control the dipole emission, enhancing either the emitted helicity or energy. Using (4.3), we obtain for the incident energy and helicity factors in the left side of (3.6) and (3.7) (we now drop the subindex i in those equations, understanding that the incident electric field is (4.3))

$$|\mathbf{E}^+(\mathbf{r})|^2 \pm |\mathbf{E}^-(\mathbf{r})|^2 = \frac{W_0^4}{16\pi\sigma^6} (|e_0^+|^2 \pm |e_0^-|^2) \left[\frac{R^2}{2} {}_1F_1^2 \left(\frac{3}{2}; 2; -\frac{R^2}{2\sigma^2} \right) + \frac{1}{k^2} {}_1F_1^2 \left(\frac{3}{2}; 1; -\frac{R^2}{2\sigma^2} \right) \right]. \quad (4.4)$$

Of course the choice of the upper or lower sign in \pm of (4.4) yields the beam energy or the helicity (cf. equation (2.12)), respectively.

Figure 2 shows the transversal intensity distribution $|\mathbf{E}^+|^2 + |\mathbf{E}^-|^2$ of this beam, given by equation (4.4) at $z = 0$, for $e_0^- = ae_0^+ \exp(ib\pi/2)$, b real, $e_0^+ = 1$ (in arbitrary units) $a = 1$, $\lambda = 589$ nm, $W_0 = 4\lambda$. This choice of the value of e_0^+ and the presence of the factor $W_0^2/4\sqrt{\pi}\sigma^3$ of the beam amplitude in (4.2) produces small values of these intensities. Also as $R^2 \gg \lambda^2$, apart from points

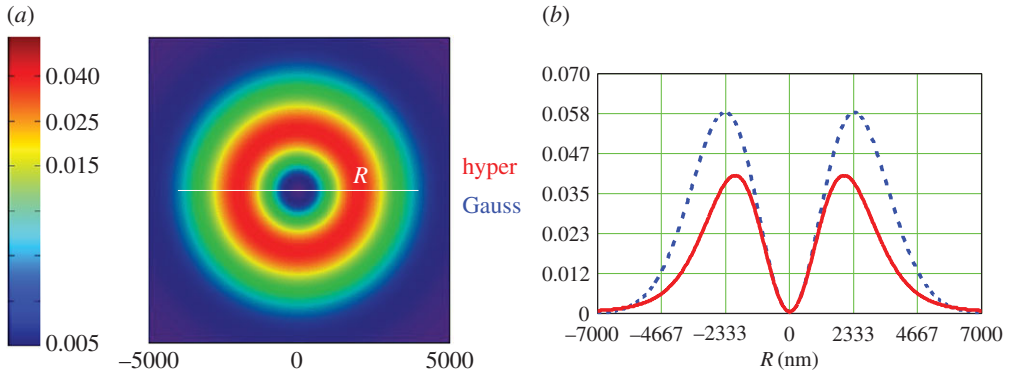


Figure 2. Intensity $|\mathbf{E}^+|^2 + |\mathbf{E}^-|^2$ (cf. equation (4.4)) at $z = 0$ of the hypergeometric beam of equation (4.3). (a) Colour map of the transversal distribution. (b) A cut of this spatial distribution as a function of the coordinate R along a diameter (full red). The distribution when the ${}_1F_1$ functions are replaced by a Gaussian of the same σ is also shown (broken blue line). (Online version in colour.)

close to $R = 0$ the second term of (4.4), given by the longitudinal component of the beam, hardly contributes to this intensity distribution. However as seen next, this longitudinal component becomes crucial when the helicity, extinguished from the incident beam and thus radiated or scattered by the particle is considered. For comparison, we also show this intensity distribution when the ${}_1F_1$ functions of (4.4) are substituted by a Gaussian with the same value of σ^2 . The difference between both distributions is small due to the similar shapes of the Gaussian and these hypergeometric functions. On the other hand, the real (and imaginary) part of the product $\mathbf{E}^- \cdot \mathbf{E}^+$ reduces to

$$\begin{Bmatrix} \Re \\ \Im \end{Bmatrix} [\mathbf{E}^- \cdot \mathbf{E}^{+*}] = \begin{Bmatrix} \Re \\ \Im \end{Bmatrix} [E_z^- \cdot E_z^{+*}] = -\frac{W_0^4}{16\pi\sigma^6 k^2} \begin{Bmatrix} \Re \\ \Im \end{Bmatrix} [e_0^- e_0^{+*}] {}_1F_1^2 \left(\frac{3}{2}; 1; -\frac{R^2}{2\sigma^2} \right). \quad (4.5)$$

So that either of these quantities, $\Re[\cdot]$ or $\Im[\cdot]$, may be made arbitrarily small (or zero) depending on the choice of parameters e_0^- and e_0^+ for the beam, which may make arbitrarily small (or zero) the factor $\begin{Bmatrix} \Re \\ \Im \end{Bmatrix} [e_0^- e_0^{+*}]$. In the next section, we show the relevance of this choice in connection with equations (3.6) and (3.7). For example, choosing as for figure 2 $e_0^-/e_0^+ = \pm a \exp(ib\pi/2)$, a and b being real, the value of $\begin{Bmatrix} \Re \\ \Im \end{Bmatrix} [\mathbf{E}^- \cdot \mathbf{E}^{+*}]$ will oscillate as $\mp \begin{Bmatrix} \cos(b\pi/2) \\ \sin(b\pi/2) \end{Bmatrix}$, thus possessing several zero values in the interval $0 \leq b \leq 4$.

Note that a kind of Hermite and Laguerre–Gaussian beam modes (m, n) are straightforwardly worked out from (4.3) on making upon $\mathbf{E}(\mathbf{r})$ the operations $\partial_x^m \partial_y^n$ and $(\partial_x + i\partial_y)^m (\partial_x - i\partial_y)^{m+n}$, respectively [36]. Likewise, Bessel beams with LCP and RCP angular components may be described by equation (4.2) using an angular spectrum $\delta(\mathbf{s} - \mathbf{s}_0)[e_0^+(\hat{\mathbf{e}}_\perp(\mathbf{s}) + i\hat{\mathbf{e}}_\parallel(\mathbf{s})) + e_0^-(\hat{\mathbf{e}}_\perp(\mathbf{s}) - i\hat{\mathbf{e}}_\parallel(\mathbf{s}))]$.

5. Example: enhancing the extinction of either chirality or energy

As an illustration of the relevance of equations (3.6) and (3.7), we consider a helical molecule with $\alpha_e^R = 1.04 \times 10^{-2} \text{ nm}^3$, $\alpha_{\text{me}}^I = 6.2 \times 10^{-5} \text{ nm}^3$, $\alpha_{\text{me}}^R = 0$, in an environment with $\epsilon = \mu = 1$ at an illumination wavelength $\lambda = 589 \text{ nm}$. $\alpha_e^I = (2/3)(2\pi/\lambda)^3 (\alpha_e^R)^2 \simeq 0.96 \cdot 10^{-10} \text{ nm}^3 \ll \alpha_e^R$, $|\alpha_m| < 10^{-5} |\alpha_e|$ [19,40].

These polarizabilities yield according to (3.6) and (3.7) for the helicity extinction $\mathcal{W}_{\mathcal{H}}^s$

$$\frac{\mu}{2\pi c} \mathcal{W}_{\mathcal{H}}^s \simeq (\alpha_e^I + \alpha_m^I)(|\mathbf{E}_i^+|^2 - |\mathbf{E}_i^-|^2) + 2(\alpha_e^R - \alpha_m^R) \Im[\mathbf{E}_i^- \cdot \mathbf{E}_i^{+*}]; \quad (5.1)$$

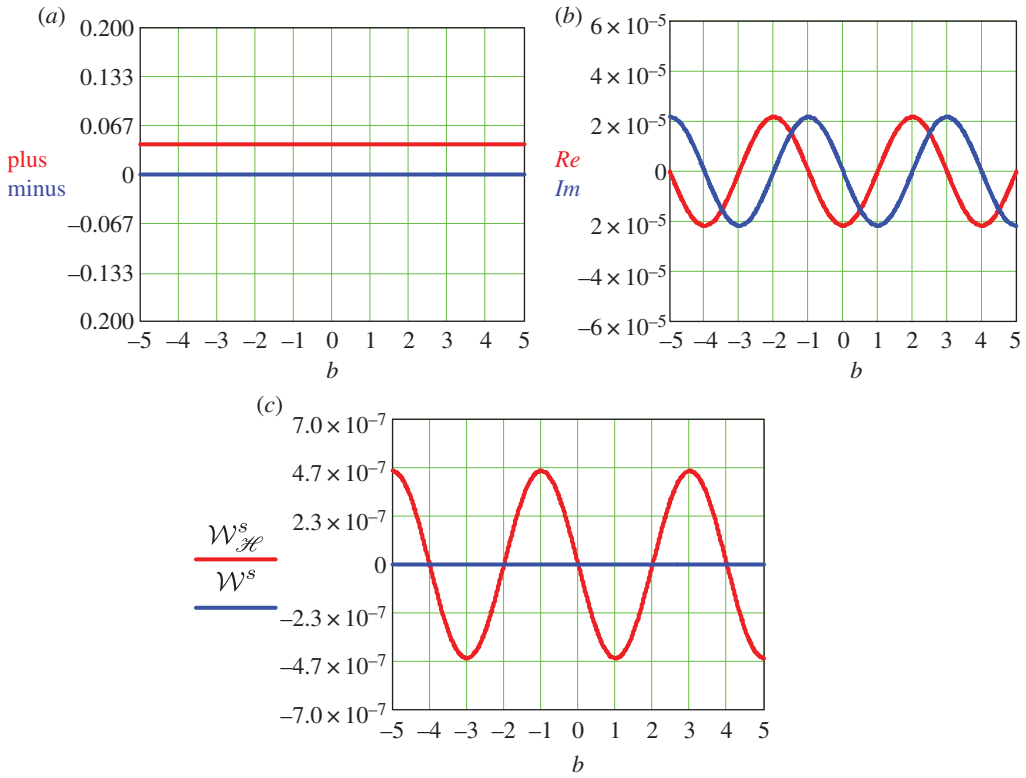


Figure 3. (a) Intensity, $plus = |\mathbf{E}^+|^2 + |\mathbf{E}^-|^2$ (red line), and helicity, $minus = |\mathbf{E}^+|^2 - |\mathbf{E}^-|^2$ (blue line) (cf. equation (4.4)), as a function of b for the hypergeometric beam of equation (4.3) at $z = 0$ and near the peak at $R = 2000$ nm (figure 2b). $e_0^- = ae_0^+ \exp(ib\pi/2)$, $e_0^+ = 1$ (in arbitrary units), $a = 1$. (b) $Re = \Re[\mathbf{E}^- \cdot \mathbf{E}^{+*}]$ and $Im = \Im[\mathbf{E}^- \cdot \mathbf{E}^{+*}]$ (cf. equation (4.5)), for the same beam and choice of parameters. (c) Extinction rate of helicity $\mathcal{W}_{\mathcal{H}}^s$ (full red) and energy \mathcal{W}^s (broken blue) in terms of b . (Online version in colour.)

and for the total emitted energy \mathcal{W}^s

$$\frac{2}{\omega} \mathcal{W}^s \simeq (\alpha_e^I + \alpha_m^I)(|\mathbf{E}_i^+|^2 + |\mathbf{E}_i^-|^2) + 2(\alpha_e^I - \alpha_m^I)\Re[\mathbf{E}_i^- \cdot \mathbf{E}_i^{+*}]. \quad (5.2)$$

We see from (5.1) that objects with such a purely imaginary α_{me} would produce no signal in a standard circular dichroism configuration, i.e. under illumination with plane CPL waves, for which $|\mathbf{E}_i^+|^2 = |\mathbf{E}_i^-|^2$, $\mathbf{E}^- \cdot \mathbf{E}^{+*} = 0$. (We recall that in such experiments the objects (molecules) usually have $\alpha_{me}^R \leq 10^{-3}\alpha_e^I$, but $\alpha_{me}^R \neq 0$.) However, impinging the particle by LCP and RCP beams with longitudinal component, like those of equation (4.3), and for example choosing as above $e_0^-/e_0^+ = \pm a \exp(ib\pi/2)$, figure 3 shows, at $R = 2000$ nm and $z = 0$, $|\mathbf{E}_i^+|^2 \pm |\mathbf{E}_i^-|^2$, as well as \Re (and \Im) of $[\mathbf{E}^- \cdot \mathbf{E}^{+*}]$ as functions of b for $W_0 = 4\lambda$, $a = 1$. The incident helicity, given by the quantity *minus* of figure 3, is zero as $|\mathbf{E}_i^+|^2 = |\mathbf{E}_i^-|^2$. As seen, the oscillations of the term $2(\alpha_e^R - \alpha_m^R)\Im[\mathbf{E}_i^- \cdot \mathbf{E}_i^{+*}]$ of (5.1) and of $2(\alpha_e^I - \alpha_m^I)\Re[\mathbf{E}_i^- \cdot \mathbf{E}_i^{+*}]$ of (5.2) lead to those of the helicity $\mathcal{W}_{\mathcal{H}}^s$ and energy \mathcal{W}^s extinction rates, respectively. The latter is constantly zero due to the very small value of the factor $(\alpha_e^I - \alpha_m^I)$ for these polarizabilities.

The corresponding quotient between $\mathcal{W}_{\mathcal{H}}^s$ and \mathcal{W}^s would be very large in this case. Therefore, this is just an illustration of how such a ratio may be enhanced depending on the constitutive parameters of the particle and choice of the beam. Other objects with different values of the polarizabilities may yield similar enhancements of either the emitted helicity—chirality—or energy depending on whether $\Im[\mathbf{E}^- \cdot \mathbf{E}^{+*}]$ dominates upon $\Re[\mathbf{E}^- \cdot \mathbf{E}^{+*}]$ in (3.6) and (3.7), or vice versa. For instance, were the ‘particle’ magnetodielectric with α_m^I comparable to α_e^R , or

just one or two orders of magnitude smaller (a difficult case to deal with conventional circular dichroism [23]), the factor $2(\alpha_e^I - \alpha_m^I)\Re[\mathbf{E}_i^- \cdot \mathbf{E}_i^{+*}]$ will give rise to an amplitude of the oscillations in \mathcal{W}^S comparable to that in $\mathcal{W}_{\mathcal{H}}^S$, or one or two orders of magnitude lower. However, the phase shift of the oscillations of $\Re[\mathbf{E}_i^- \cdot \mathbf{E}_i^{+*}]$ and $\Im[\mathbf{E}_i^- \cdot \mathbf{E}_i^{+*}]$ (cf. *Re* and *Im* in figure 3) allows us to tailor the beam, producing an enhancement of $\mathcal{W}_{\mathcal{H}}^S$ or of \mathcal{W}^S .

6. Concluding remarks

Based on a recent optical theorem put forward for the electromagnetic helicity, or chirality, extinction rate of quasi-monochromatic wavefields [16], which characterizes the emitted or scattered helicity by extinction of that of the incident field, we have demonstrated that dichroism is not only a manifestation of molecular absorption, but it is a universal phenomenon which appears in the scattering or diffraction of twisted waves. This provides a general basic answer to the question on the conditions under which an object produces chiral fields and/or dichroism, and whether a chiral scatterer is required to produce such effect.

In this respect, we have established that both dichroism and chirality of emitted or scattered wavefields from wide sense dipolar particles are consequences of the helicity of the illumination, or of the mutual relationship between the emitting electric and magnetic dipoles; but these phenomena do not require the object constitutive parameters, refractive indices and polarizabilities, to be those of a chiral structure. For example, as we have shown, to obtain a circularly polarized emitted or scattered field, it is a sufficient condition that the particle-induced electric and magnetic dipoles rotate and differ from each other by only a $\pm\pi/2$ phase; but no chiral cross-polarizability α_{me} is necessary. Thus, an achiral particle ($\alpha_{me} = 0$) may produce dichroism on scattering of a chiral incident wave. Henceforth, the standard concept of circular dichroism is generalized to include fields with both LCP and RCP components and a net helicity.

Based on the angular spectrum representation, we have introduced new families of optical beams with right-circular and left-circular polarization, and with longitudinal components. Tailoring these fields, used in our optical theorem as incident waves on the scattering particle, overcomes previous limitations of circular dichroism without needing to place nearby additional objects to enhance the signal [29,30,41]. Depending on the parameters chosen for these beams, the enhancement of the extinction rate of helicity and/or of energy is produced, i.e. the dichroism scattered signal is either augmented or lowered. This not only provides a new procedure for object (and particularly enantiomeric) characterization on illumination with twisted beams, but it also yields a way of controlling the helicity and energy of radiated wavefields by using such scattering particles as secondary sources.

Competing interests. I declare I have no competing interests.

Funding. Work supported by MINECO, grant nos. FIS2012-36113-C03-03, FIS2014-55563-REDC and FIS2015-69295-C3-1-P.

Acknowledgements. The author thanks Dr J. M. Auñón for a critical reading of the manuscript and helpful comments.

References

1. Richardson FS, Riehl JP. 1977 Circularly polarized luminescence spectroscopy. *Chem. Rev.* **77**, 773–792. (doi:10.1021/cr60310a001)
2. Allen L, Barnett SM, Padgett MJ (eds). 2003 *Optical angular momentum*. Bristol, UK: IOP Publishing.
3. Allen L, Padgett MJ, Babiker M. 1999 The orbital angular momentum of light. In *Prog. Opt.*, (ed E. Wolf) vol. 39, Amsterdam, The Netherlands: Elsevier.
4. Tang Y, Cohen AE. 2010 Optical chirality and its interaction with matter. *Phys. Rev. Lett.* **104**, 163901. (doi:10.1103/PhysRevLett.104.163901)
5. Tang Y, Cohen AE. 2011 Enhanced enantioselectivity in excitation of chiral molecules by superchiral light. *Science* **332**, 333–336. (doi:10.1126/science.1202817)

6. Cameron RP, Barnett SM, Yao AM. 2012 Optical helicity, optical spin and related quantities in electromagnetic theory. *New J. Phys.* **14**, 053050. (doi:10.1088/1367-2630/14/5/053050)
7. Riehl JP, Muller G. 2012. Circularly polarized luminescence spectroscopy and emission-detected circular dichroism. In *Comprehensive Spectroscopy*, (eds N Berova, PL Polavarapu, K Nakanishi, RW Woody) vol. 1., Ch. 3. Hoboken, NJ: J. Wiley.
8. Andrews DL, Babiker M (eds). 2013 *The angular momentum of light*. Cambridge, UK: Cambridge University Press.
9. Cameron RP, Gotte JB, Barnett SM. 2015 Chiral rotational spectroscopy. (<http://arxiv.org/abs/1511.04615v1>)
10. Andrews DL, Coles MM. 2012 Photonic measures of helicity: optical vortices and circularly polarized reflection. *Opt. Lett.* **38**, 869–871.
11. Andrews DL, Coles MM, Williams MD, Bradshaw DS. 2013 Expanded horizons for generating and exploring optical angular momentum in vortex structures.. *Proc. SPIE* **8813**, 88130Y. (doi:10.1117/12.2025141)
12. O'Sullivan MN, Mirhosseini M, Malik M, Boyd RW. 2012 Near-perfect sorting of orbital angular momentum and angular position states of light. *Opt. Express* **20**, 24444–24449. (doi:10.1364/OE.20.024444)
13. Krenn M, Tischler N, Zeilinger A. 2016 On small beams with large topological charge. *New J. Phys.* **18**, 033012–033019. (doi:10.1088/1367-2630/18/3/033012)
14. Lipkin DM. 1964 Existence of a new conservation law in electromagnetic theory. *J. Math. Phys.* **5**, 696–700. (doi:10.1063/1.1704165)
15. Bliokh KY, Nori F. 2011 Characterizing optical chirality. *Phys. Rev. A* **83**, 021803. (doi:10.1103/PhysRevA.83.021803)
16. Nieto-Vesperinas M. 2015 Optical theorem for the conservation of electromagnetic helicity: significance for molecular energy transfer and enantiomeric discrimination by circular dichroism. *Phys. Rev. A* **92**, 023813. (doi:10.1103/PhysRevA.92.023813)
17. Schellman JA. 1975 Circular dichroism and optical rotation. *Chem. Rev.* **75**, 323–331. (doi:10.1021/cr60295a004)
18. Craig DP, Thirunamachandran T 1998 *Molecular quantum electrodynamics: an introduction to radiation molecule interactions*. New York, NY: Dover.
19. Barron LD 2004 *Molecular light scattering and optical activity*. Cambridge, UK: Cambridge University Press.
20. Zambrana-Puyalto X, Vidal X, Molina-Terriza G. 2014 Angular momentum-induced circular dichroism in non-chiral nanostructures. *Nat. Commun.* **5**, 4922. (doi:10.1038/ncomms5922)
21. Poulidakos LV, Gutsche P, McPeak KM, Burger S, Niegemann J, Hafner C, Norris DJ. 2016 Optical chirality flux as a useful far-field probe of chiral near fields. *ACS Photonics* **3**, 1619–1625. (doi:10.1021/acsphotonics.6b00201)
22. Gutsche P, Poulidakos LV, Hammerschmidt M, Burger S, Schmidt F. 2016 Time-harmonic optical chirality in inhomogeneous space. (<http://arxiv.org/abs/1603.05011v1>)
23. Choi JS, Cho M. 2012 Limitations of a superchiral field. *Phys. Rev. A* **86**, 063834. (doi:10.1103/PhysRevA.86.063834)
24. Kong JA 1972. *Proc. IEEE* **60**, *Theorems of bianisotropic Media*, 1036–1046.
25. Nieto-Vesperinas M. 2015 Optical torque: electromagnetic spin and orbital-angular-momentum conservation laws and their significance. *Phys. Rev. A* **92**, 043843. (doi:10.1103/PhysRevA.92.043843)
26. Bohren CF, Huffman DR. 1983 *Absorption and scattering of light by small particles*. New York, NY: J. Wiley.
27. Born M, Wolf E. 1999 *Principles of optics*, 7th edn. Cambridge, UK: Cambridge University Press.
28. Novotny L, Hecht B. 2012 *Principles of nano-optics*, 2nd edn. Cambridge, UK: Cambridge University Press.
29. Guzatov DV, Klimov VV. 2012 The influence of chiral spherical particles on the radiation of optically active molecules. *New J. Phys.* **14**, 123009. (doi:10.1088/1367-2630/14/12/123009)
30. Alaeian H, Dionne JA. 2015 Controlling electric, magnetic, and chiral dipolar emission with PT-symmetric potentials. *Phys. Rev. B* **91**, 245108. (doi:10.1103/PhysRevB.91.245108)
31. Jackson JD. 1998 *Classical electrodynamics*, 3rd edn. New York, NY: John Wiley.
32. Mandel L, Wolf E. 1995 *Optical coherence and quantum optics*. Cambridge, UK: Cambridge University Press.

33. Nieto-Vesperinas M. 2006 *Scattering and diffraction in physical optics*, 2nd edn. Singapore: World Scientific.
34. Crichton JH, Marston PL. 2000. The measurable distinction between the spin and orbital angular momenta of electromagnetic radiation. *Electron. J. Dif. Eqs. Conf.* 04, 37. See <http://ejde.math.swt.edu> or <http://ejde.math.unt.edu>.
35. Berry MV. 2009 Optical currents. *J. Opt. A* **11**, 094001–094012. (doi:10.1088/1464-4258/11/9/094001)
36. Zauderer E. 1986 Complex argument Hermite-Gaussian and Laguerre-Gaussian beams. *J. Opt. Soc. Am. A* **3**, 465–469. (doi:10.1364/JOSAA.3.000465)
37. Gradshteyn IS, Ryzhik IM 2007. *Table of integrals, series, and products* (eds A Jeffrey, D Zwillinger), 7th edn. New York, NY: Academic Press.
38. Abramowitz M, Stegun I 1972. *Handbook of mathematical functions*. National Bureau of Standards, Applied Mathematical Series vol. 25, 3rd Printing, Washington, DC.
39. Karimi E, Zito G, Piccirillo B, Marrucci L, Santamato E. 2007 Hypergeometric-gaussian modes. *Opt. Lett.* **32**, 3053–3055. (doi:10.1364/OL.32.003053)
40. Hayat A, Mueller JPB, Capasso F. 2016 Lateral chirality-sorting optical forces. *Proc. Natl Acad. Sci. USA* **112**, 13 190–13 194. (doi:10.1073/pnas.1516704112)
41. Krasnok A, Glybovski S, Petrov M, Makarov S, Savelev R, Belov P, Simovski C, Kivshar Y. 2016 Demonstration of the enhanced Purcell factor in all-dielectric structures. *Appl. Phys. Lett.* **108**, 211 105–211 108. (doi:10.1063/1.4952740)